1   **Title: Fully oxygenated water columns over continental shelves before the Great Oxidation**

2   **Event**

3

4   **Authors:** Chadlin M. Ostrander[1,2,*], Sune G. Nielsen[2,3], Jeremy D. Owens[4], Brian Kendall[5],

5   Gwyneth W. Gordon[1], Stephen J. Romaniello[1], and Ariel D. Anbar[1]

6

7   **Affiliations:**

8   [1]School of Earth and Space Exploration, Arizona State University, Tempe, AZ, USA

9   [2]NIRVANA Laboratories, Woods Hole Oceanographic Institution, Woods Hole, MA, USA

10   [3]Department of Geology and Geophysics, Woods Hole Oceanographic Institution, Woods Hole,

11   MA, USA

12   [4]Department of Earth, Ocean, and Atmospheric Science, National High Magnetic Field

13   Laboratory, Florida State University, Tallahassee, FL, USA

14   [5]Department of Earth and Environmental Sciences, University of Waterloo, Waterloo, Ontario,

15   CA

16   [6]School of Molecular Sciences, Arizona State University, Tempe, AZ, USA

17

18   **Late Archaean sedimentary rocks contain compelling geochemical evidence for episodic**

19   **accumulation of dissolved oxygen in the oceans along continental margins before the Great**

20   **Oxidation Event. However, the extent of this oxygenation remains poorly constrained. Here**

21   **we present thallium and molybdenum isotope compositions for anoxic organic-rich shales**

22   **of the 2.5 billion-year-old Mount McRae Shale from Western Australia, which previously**

23   **yielded geochemical evidence of a transient oxygenation event. During this event, we**

24 **observe an anti-correlation between thalium and molybdenum isotope data, including two**

25 **shifts to higher molybdenum and lower thalium isotope compositions. Our data indicate**

26 **pronounced burial of manganese oxides in sediments elsewhere in the ocean at these times,**

27 **which requires that water columns above portions of the ocean floor were fully oxygenated:**

28 **all the way from the air-sea interface to well below the sediment-water interface. Well-**

29 **oxygenated continental shelves were likely the most important sites of manganese oxide**

30 **burial and mass-balance modeling results suggest that fully oxygenated water columns**

31 **were at least a regional-scale feature of early-Earth's oceans 2.5 billion years ago.**

32

33   The extent of dissolved O_2 accumulation in Earth's oceans before the Great Oxidation

34 Event remains poorly understood (GOE; ~2.4 to 2.3 Ga[1]). Multiple lines of geochemical

35 evidence indicate that O_2 was produced by cyanobacteria in the surface ocean well before

36 accumulating in the atmosphere during and after the GOE[2-8]. Models indicate that cyanobacteria

37 in the surface ocean were capable of promoting mild accumulation of dissolved O_2 (up to 25

38 μM[9]) in shallow waters under a predominately anoxic atmosphere, perhaps extending across

39 large areas of the ocean[10]. However, it is difficult to test these models because existing

40 geochemical proxies cannot easily be used to assess the breadth and depth of ocean oxygenation.

41   A case has been made for widespread oxygenation of shallow waters before the GOE in

42 continental margin environments based on carbon isotopes in bulk rock and kerogen from 2.7 Ga

43 carbonate sedimentary rocks[2]. However, this prior work could not determine whether O_2

44 accumulation was restricted to surface waters or if it extended deeper in the water column, let

45 alone whether oxygenation reached bottom-waters and sediments (i.e., a fully oxygenated water

46 column).

47   A fully oxygenated water column at 2.6–2.5 Ga was inferred from black shales (upper

48   Nauga Formation, Ghaap Group, South Africa) enriched in Re but not Mo relative to average

49   crustal abundances[3]. This geochemical signature occurs when O_2 is present in pore waters at a

50   depth of up to about one centimeter below the sediment-water interface, when Fe(III) becomes

51   the dominant electron acceptor during organic matter oxidation and sulfide accumulation is

52   low[11,12] (Figure 1, panel A). However, this evidence was restricted to a single continental margin

53   (Griqualand West Basin) and could not be extrapolated to the wider oceans.

54   If fully oxygenated water columns on continental margins were a widespread feature of

55   pre-GOE oceans, then Mn oxide burial in sediments beneath these settings would also have been

56   widespread. In the modern ocean, O_2 in marine bottom waters and sediments readily oxidizes

57   dissolved Mn(II) and Mn(III) to insoluble Mn(IV)-bearing minerals that precipitate out of

58   solution[13,14]. In contrast, Mn oxides do not form under anoxic conditions, nor are they buried in

59   anoxic marine sediments. Even if formed under O_2-rich conditions, Mn oxides undergo reductive

60   dissolution shortly after being exposed to anoxic conditions within the water column or

61   sediments[13-15]. Manganese oxides are highly unstable when O_2 is absent because in such

62   conditions they are an efficient electron acceptor[16]. Therefore, appreciable Mn oxide burial today

63   only occurs where water columns are fully oxygenated and O_2 persistently penetrates sediment

64   pore waters[14]. In Earth's past, Mn oxides should have also been buried where O_2 penetrated

65   deeply into marine sediments. This could have occurred under more oxidizing conditions than

66   those identified by Kendall et al. (2010) in the Nauga Formation shales, where Re abundances

67   are elevated but Mo abundances are negligible. Specifically, Mn oxide burial requires

68   penetration of O_2 well beyond one centimeter below the sediment water interface and occurs

69   before Fe(III) becomes the primary electron acceptor during organic carbon oxidation[14,16] (e.g.,

70   Figure 1, Panel B).

71   Here, we pair Tl and Mo isotope data from the late Archaean (~2.5 Ga) black shales of

72   the Mt. McRae Shale (Hamersley Basin, Western Australia) to track the extent of marine Mn

73   oxide burial before the GOE. The isotopic cycling of both Tl and Mo in the ocean is directly

74   linked to global Mn oxide burial fluxes[17,18]. Therefore, their paired application is a powerful way

75   to infer the extent of fully oxygenated water columns at a regional-to-global scale, in contrast to

76   other proxies (e.g., Re vs Mo enrichments and[11] sedimentary Fe speciation[19]) that focus only on

77   redox conditions in the local water column.

78

79   **Pairing Tl and Mo isotopes to track paleoredox conditions**

80   The use of Tl isotopes as a paleoredox proxy is relatively new[17,20,21], but builds on

81   extensive prior study of Tl isotope systematics. The Tl isotope composition of modern seawater

82   [reported in epsilon notation: $\varepsilon^{205}Tl$, where $\varepsilon^{205}Tl = (^{205/203}Tl_{sample}/^{205/203}Tl_{NIST-997} - 1) \cdot 10^4$] is

83   homogenous and lighter than that of bulk continental crust ($\varepsilon^{205}Tl_{seawater} = -6.0 \pm 0.3^{[18,22]}$,

84   compared to $\varepsilon^{205}Tl_{bulk-crust} = -2.1 \pm 0.3^{[23]}$). The light $\varepsilon^{205}Tl$ in modern seawater is a result of

85   preferential removal of isotopically heavy Tl from seawater by Mn oxides in well-oxygenated

86   marine sediments[24]. Importantly, the contemporaneous seawater $\varepsilon^{205}Tl$ signature is captured and

87   preserved in sediments from anoxic and sulfidic (i.e. euxinic) basins[18]. Therefore, Tl isotope

88   studies of sedimentary rocks deposited under euxinic conditions provide a means to track ancient

89   seawater $\varepsilon^{205}Tl$ signatures, which should vary in response to changes in Mn oxide burial fluxes.

90   In support of this application, two recent studies used Tl isotope compositions in Mesozoic

91   shales deposited in locally euxinic conditions to track changes in Mn oxide burial fluxes before,

92   during, and after Oceanic Anoxic Events, documenting episodes of significant marine

93   deoxygenation[20,21].

94   Molybdenum isotopes are a more established proxy also shown to be sensitive to marine

95   Mn oxide burial[25]. The modern seawater Mo isotope composition [reported in delta notation:

96   $\delta^{98}Mo$, where $\delta^{98}Mo = ((^{98/95}Mo_{sample}/^{98/95}Mo_{NIST-SRM-3134} - 1) \cdot 10^3) + 0.25‰^{[26]}$] is heavier than

97   that of bulk continental crust ($\delta^{98}Mo_{seawater} = 2.34 \pm 0.10‰^{[26]}$, compared to $\delta^{98}Mo_{bulk-crust} = 0.47$

98   $\pm 0.12‰^{[27]}$). This heavy seawater $\delta^{98}Mo$ composition is due largely to preferential removal of

99   lighter-mass Mo isotopes by adsorption to Mn oxides in well-oxygenated marine sediments[25].

100 Similar to Tl, this heavy seawater $\delta^{98}Mo$ value is captured in strongly euxinic settings where Mo

101 removal from bottom waters is nearly quantitative[28].

102   It is advantageous to measure Tl isotopes in addition to Mo isotopes because Mo isotope

103 interpretation is complicated by alternative fractionation pathways that do not affect Tl isotopes.

104 For example, processes that occur during continental weathering[29] and riverine transport[30] can

105 remove isotopically light Mo (but see reference 31), but do not cause measurable Tl isotope

106 fractionation[23]. Weakly sulfidic marine sediments also incorporate lighter-mass Mo isotopes[28]

107 but impart no known isotopic effect on Tl[18]. Iron oxides can remove isotopically light Mo and

108 drive seawater to heavy $\delta^{98}Mo$ values[32], but are unlikely to fractionate Tl isotopes because Fe

109 oxides lack the ability to oxidize Tl(I) to Tl(III), which is what drives isotopic fractionation

110 during sorption to Mn oxides[24,33]. This study is the first to pair both proxies in the same sample

111 set.

112

113 **Anti-correlation of Mo and Tl isotopes in the Mt. McRae Shale**

114   We focus on the 2.5 Ga Mt. McRae Shale from Western Australia in drill core ABDP9

115   because black shales from the upper part of this formation host convincing evidence for a

116   widespread oxygenation episode predating the GOE[5,6,34-40]. These rocks are an ideal archive for

117   tracking fluctuations in seawater Tl and Mo isotope compositions at 2.5 Ga because they were

118   deposited in locally euxinic conditions[37] that favor preservation of seawater δ^{98}Mo and ε^{205}Tl

119   values (Figure 1; see supplement for more information about the Mt. McRae Shale).

120   Molybdenum isotope signatures much heavier than those in igneous crustal rocks were

121   previously found in the Mt. McRae Shale (and in coeval shales from South Africa[41]) but could

122   not be definitively ascribed to Mn oxide burial elsewhere in the ocean[38]. If Mn oxides were being

123   buried at this time, ε^{205}Tl should also be fractionated relative to bulk continental crust. An anti-

124   correlation between ε^{205}Tl and δ^{98}Mo is expected because fractionation incurred during Mn oxide

125   adsorption is in opposing directions for the two isotope systems[17,18].

126   We find that ε^{205}Tl is systematically lighter during two distinct intervals of the euxinic

127   upper shale (US) member in the Mt. McRae Shale: 153.30-144.36 m (US1) and 134.17-126.15 m

128   (US3) (average ε^{205}Tl = -2.65) (Figure 2). δ^{98}Mo exhibits heavier values in these same intervals

129   (average δ^{98}Mo = 1.37‰), revealing the predicted anti-correlation with ε^{205}Tl. Compared to

130   these intervals, Tl and Mo isotope compositions for 144.26-135.58 m (US2) are heavier (average

131   ε^{205}Tl = -2.39, p-value = 0.05, two-tailed unpaired t-test) and lighter (average δ^{98}Mo = 1.23‰, p-

132   value << 0.05), respectively. A cross-plot of shale samples with both isotope measurements from

133   the US reveals a statistically significant anti-correlation (p-value = 0.01). In contrast to the

134   euxinic US, isotope compositions are invariant in the non-euxinic lower shale member (170-190

135   m core depth, see supplement for discussion of this interval, and interpretation of concentration

136   data).

137

Fully oxygenated regional water columns on continental shelves

139   Light ε^{205}Tl and heavy δ^{98}Mo in US1 and US3 provide strong evidence for the formation

140   and subsequent burial of Mn oxides elsewhere in the ocean at these times. To drive the observed

141   isotopic trends, water columns needed to have been fully oxygenated over portions of the ocean

142   floor. Most likely, Mn oxide burial at 2.5 Ga occurred in shallow oxygenated shelf environments

143   where O_2 produced within the surface ocean by cyanobacteria was capable of being continuously

144   transferred to underlying waters and marine sediments (e.g., the environment illustrated in Figure

145   1).

146   Alternative local basin controls or processes in the sedimentary environment where the

147   Mt. McRae Shale was deposited cannot explain the observed isotope trends in the upper shale

148   member. In a modern euxinic basin that is not well-connected to the open ocean (i.e., the Black

149   Sea), Tl isotopes in the local water column and underlying sediments are heavier than the open-

150   ocean signature[18]. If the Hamersley Basin was also not well-connected to the open-ocean, then

151   ε^{205}Tl of the Mt. McRae Shale may have been higher than the open-ocean signature. This would

152   require even lighter seawater ε^{205}Tl compositions during deposition of US1 and US3, which

153   would then imply an even greater extent of sediment Mn oxide burial elsewhere in the oceans.

154   Furthermore, in modern euxinic settings where Mo is not quantitatively transferred from

155   seawater to sediments, sedimentary δ^{98}Mo compositions are always lighter than the coeval

156   seawater signature[28]. Hence, if Mo removal from euxinic bottom waters in the Hamersley Basin

157   was not quantitative, then seawater δ^{98}Mo would be even heavier than observed in the Mt.

158   McRae Shale, again implying even more significant sediment Mn oxide burial elsewhere in the

159   ocean.

160   In theory, the observed Tl and Mo isotope shifts might be alternatively explained by

161   "shuttling" of Tl and Mo bound to oxide minerals formed in oxic surface waters to underlying

162   anoxic waters and/or sediments on Late Archaean continental margins, where these elements

163   could then be captured in euxinic sediments. If so, fully oxygenated water columns would not be

164   required to explain the antithetic shifts in Tl and Mo isotopes recorded in the Mt. McRae Shale.

165   However, this notion is not supported by observations in the modern Cariaco Basin, a modern

166   analog environment where Mn oxides are formed in oxygenated surface waters and subsequently

167   transported to euxinic bottom waters and sediments deeper in the basin[42]. An oxide shuttle

168   should cause ε^{205}Tl in euxinic sediments to be heavier than in surface oxic seawater[24]. This is not

169   observed, however. Rather, euxinic sediment ε^{205}Tl in the Cariaco Basin is indistinguishable

170   from overlying seawater (average ε^{205}Tl$_{euxinic}$ = -5.1 ± 1.3; 2SD vs. ε^{205}Tl$_{seawater}$ -5.5 ± 0.7;

171   2SD)[18]. One possible explanation for this lack of Tl isotope is that Tl released by Mn oxide

172   dissolution in sulfidic deep waters is first re-mixed and re-homogenized with the dissolved Tl

173   pool prior to Tl capture in pyrite. Regardless, since anoxic sediments in the modern Cariaco

174   Basin *do not* preserve the Tl isotope effects of oxide adsorption[18] even though oxide minerals are

175   shown to be delivered at least transiently to these sediments[42], a Mn oxide shuttle in redox-

176   stratified marine basins probably had a minimal impact on the Late Archaean seawater Tl isotope

177   mass-balance.

178   Although there are proposed pathways of Mn oxide formation that do not require O_2, they

179   would not be likely to cause the observed isotopic effects in the upper shale member. Oxidation

180   of reduced Mn in the upper water column by hypothesized Mn-oxidizing phototrophs[43] or by UV

181   light[44] cannot account for burial at the seafloor because underlying anoxic waters and sediments

182   would recycle Mn back into solution [as Mn(II)][13,14]. The high abundance of Fe(II) in deep

183 ferruginous waters of the Archaean oceans[1], for example, would readily promote reduction of

184 Mn oxides in anoxic waters. If the water column or sediment pore waters were anoxic, even

185 seasonally[15], reductive dissolution of Mn oxides would release sorbed Tl and Mo. Additionally,

186 invoking an O_2-free explanation to explain the observed isotopic trends requires neglecting the

187 many independent lines of evidence for a "whiff" of O_2 at 2.5 Ga[5,6,34-40].

188 Paleo-seawater ε^{205}Tl and δ^{98}Mo can be estimated directly from the Mt. McRae Shale

189 data and used to reconstruct ocean redox conditions. Measured ε^{205}Tl values serve as a direct

190 estimate for the coeval seawater signature (as low as -3.57 ± 0.48) because euxinic sediments

191 capture the overlying seawater Tl isotope value[18]. The δ^{98}Mo recorded in euxinic marine

192 sediments is always equal to or lighter than seawater[28], and thus represent a lower limit for the

193 coeval seawater signature (as heavy as 1.56 ± 0.10‰). It is possible, indeed likely, that the Tl

194 and Mo isotope compositions of seawater fluctuated during deposition of the US member of the

195 Mt. McRae Shale. Deposition of this interval is estimated to have occurred over ~11 million

196 years[34] and the "whiff" of O_2 was likely a transient episode of even shorter duration[39]. To

197 estimate ocean redox conditions during peak Mn oxide burial, we use the lightest ε^{205}Tl and

198 heaviest δ^{98}Mo from the US member. During peak Mn oxide burial, retention of heavier-mass Tl

199 and lighter-mass Mo isotopes would have been maximized, resulting in the lightest ε^{205}Tl and

200 heaviest δ^{98}Mo seawater signatures. Unsurprisingly, the lightest ε^{205}Tl (-3.57 ± 0.48 epsilon units

201 at 148.75 m) and heaviest δ^{98}Mo (1.56 ± 0.10‰ at 145.74 m) occur during US1, an interval that

202 hosts multiple lines of geochemical evidence for an oxygenation episode[5,6,34,37-39].

203 Using the estimated seawater ε^{205}Tl and δ^{98}Mo, ocean redox conditions can be inferred

204 using isotope mass-balance equations as follows:

205 $\varepsilon^{205}\text{Tl}_{\text{Inputs}} = \varepsilon^{205}\text{Tl}_{\text{AOC}}(f_{\text{AOC}}) + \varepsilon^{205}\text{Tl}_{\text{oxic}}(f_{\text{Tl-oxic}}) + \varepsilon^{205}\text{Tl}_{\text{other}}(f_{\text{other}})$

206   and

207    $\delta^{98}Mo_{Inputs} = \delta^{98}Mo_{euxinic}(f_{euxinic}) + \delta^{98}Mo_{SAD}(f_{SAD}) + \delta^{98}Mo_{oxic}(f_{Mo\text{-}oxic})$

208   where $\varepsilon^{205}Tl_x$ and $\delta^{98}Mo_x$ represent the isotopic composition of average oceanic inputs and

209   outputs, and f_x denotes the relative removal flux for each output. For Tl, we designate low-T

210   alteration of oceanic crust (f_{AOC}), well-oxygenated Mn oxide-rich sediments ($f_{Tl\text{-}oxic}$), and "other"

211   (f_{other}) as the three dominant marine outputs. The "other" output signifies Tl removal with no

212   associated isotopic fractionation (e.g., euxinic basins[18]). For Mo, similar to recent work, we use

213   euxinic sediments ($f_{euxinic}$), sediments that are sulfidic at depth (f_{SAD}; where sulfide is limited to

214   sediment pore waters), and well-oxygenated Mn oxide-rich sediments ($f_{Mo\text{-}oxic}$) as the three

215   outputs[45] (see supplementary material for more detailed information about modeling, including

216   key assumptions).

217   The mass-balance model results indicate that well-oxygenated Mn oxide-rich sediments

218   were an important sink for both Tl ($f_{Tl\text{-}oxic}$ = 6-21%) and Mo ($f_{Mo\text{-}oxic}$ = 20-34%) at 2.5 Ga.

219   Together, these results suggest that fully oxygenated shelf environments were a common feature

220   on continental margins, at least regionally at 2.5 Ga.

221   We make no attempt here to convert these fluxes into the areal extent of seafloor because

222   the flux per areal unit into these marine outputs was likely much different in the Archean

223   compared to today. Burial rates of Tl and Mo in modern oxic marine environments that bury Mn

224   oxides are very low, much lower than their burial rates into other modern marine outputs (e.g.,

225   burial of Tl during low-T alteration of oceanic crust[46] and burial of Mo under strong euxinic

226   conditions[45]). For this reason, seafloor area calculations using modern Tl and Mo burial rates and

227   our ancient seawater isotope signature estimates would require the majority of the seafloor at 2.5

228   Ga to have been oxic. Expansive oxic conditions before the GOE is unlikely because many

229   independent lines of evidence support a predominately anoxic global ocean at this time[1]. Most

230   likely, burial rates of Tl and Mo in 2.5 Ga oxic environments were much higher than today. For

231   example, dissolved Mn concentrations in Archean seawater may have been four orders of

232   magnitude higher than today[47], providing a strong potential for high Mn oxide burial rates in oxic

233   environments, and therefore a stronger potential for Tl and Mo adsorption. Furthermore, the

234   burial rate of Mo (and potentially also of Tl) into euxinic environments could have been much

235   lower than today because sulfate concentrations in Archean oceans were very low[48]. Euxinic

236   conditions in a low-sulfate ocean could have been much weaker than today, lowering the

237   potential for sedimentary retention of Mo. In summary, a smaller area of 2.5 Ga seafloor burying

238   Mn oxides could conceivably drive a more pronounced seawater Tl and Mo isotope signature

239   effect than today but is difficult to estimate precisely.

240   Our findings provide a new perspective on marine oxygenation at 2.5 Ga, on the eve of

241   the GOE. Multiple lines of geochemical evidence provide strong support for O_2 in shallow

242   waters of the Hamersley Basin at 2.5 Ga[5,6,34] and the adjoining Griqualand West Basin[4,41] (which

243   may have bordered the same ocean basin[49]). However, because Mn oxide burial requires fully

244   oxygenated water columns at 2.5 Ga, our multi-isotope data supports more oxygenated

245   continental shelves over a greater area than previously recognized using other geochemical

246   datasets. Specifically, the inferred seawater ε^{205}Tl and δ^{98}Mo requires fully oxygenated water

247   columns in shelf environments within the Hamersley Basin and adjoining basins(s), and

248   potentially even large portions of the continental margins worldwide. Our results highlight the

249   significant and expanding role of cyanobacteria as engineers of the Archean biosphere,

250   particularly in the runup to the Great Oxidation Event.

251

252   **References:**

253   1. Lyons, T. W., Reinhard, C. T. & Planavsky, N. J. The rise of oxygen in Earth's early ocean

254   and atmosphere. *Nature* **506,** 307-315 (2014).

255   2. Eigenbrode, J. L. & Freeman, K. H. Late Archean rise of aerobic microbial ecosystems.

256   *Proc. Natl. Acad. Sci.* **103,** 15759-15764 (2006).

257   3. Kendall, B. et al. Pervasive oxygenation along late Archaean ocean margins. *Nat. Geosci.* **3,**

258   647-652 (2010).

259   4. Czaja, A. D. et al. Evidence for free oxygen in the Neoarchean ocean based on coupled iron-

260   molybdenum isotope fractionation. *Geochim. Cosmochim. Acta* **86,** 118-137 (2012).

261   5. Kendall, B., Brennecka, G. A., Weyer, S. & Anbar, A. D. Uranium isotope fractionation

262   suggests oxidative uranium mobilization at 2.50 Ga. *Chem. Geol.* **362,** 105-114 (2013).

263   6. Stüeken, E. E., Buick, R. & Anbar, A. D. Selenium isotopes support free O_2 in the latest

264   Archean. *Geology* **43,** 259-262 (2015).

265   7. Eickmann, B. et al. Isotopic evidence for oxygenated Mesoarchaean shallow oceans. *Nat.*

266   *Geosci.* **11,** 133-138 (2018).

267   8. Koehler, M. C., Buick, R., Kipp, M. A., Stüeken, E. E. & Zaloumis, J. Transient surface

268   ocean oxygenation recorded in the ~2.66-Ga Jeerinah Formation, Australia. *Proc. Natl. Acad.*

269   *Sci.* **115,** 7711-7716 (2006).

270   9. Kasting, J. F. Models relating to Proterozoic atmospheric and ocean chemistry. In: Schopf, J.,

271   Klein, C. (Eds), *The Proterozoic Biosphere, A Multidisciplinary Study*. Cambridge

272   University Press, 1185-1187 (1992).

273   10. Olson, S. L., Kump, L. R. & Kasting, J. F. Quantifying the areal extent and dissolved oxygen

274   concentrations of Archean oxygen oases. *Chem. Geol.* **362,** 35-43 (2013).

275   11. Morford, J. L., Emerson, S. R., Breckel, E. J. & Kim, S. H. Diagenesis of oxyanions (V, U,

276   Re, and Mo) in pore waters and sediments from a continental margin. *Geochim. Cosmochim.*

277   *Acta* **69,** 5021-5032 (2005)

278   12. Morford, J. L., Martin, W. R. & Carney, C. M., Rhenium geochemical cycling: Insights from

279   continental margins. *Chem. Geol.* **324-325,** 73-86 (2012)

280   13. Burdige, D. J. The biogeochemistry of manganese and iron reduction in marine sediments.

281   *Earth Sci. Rev.* **35,** 249-284 (1993).

282   14. Calvert, S. E. & Pedersen, T. F. Sedimentary Geochemistry of Manganese: Implications for

283   the environment of formation of manganiferous black shales. *Econ. Geol.* **91,** 36-47 (1996).

284   15. Kristensen, E. Kristiansen, K. D. & Jensen, M. H. Temporal behavior of Manganese and Iron

285   in a Sandy Coastal Sediment Exposed to Water Column Anoxia. *Estuaries* **26,** 690-699

286   (2003).

287   16. Froelich, P. N. et al. Early oxidation of organic matter in pelagic sediments of the eastern

288   equatorial Atlantic: Suboxic diagenesis. *Geochim. Cosmochim. Acta* **43,** 1075–1090 (1979).

289   17. Nielsen, S. G. et al. Thallium isotopes in early diagenetic pyrite – A paleoredox proxy?

290   *Geochim. Cosmochim. Acta* **75,** 6690-6704 (2011).

291   18. Owens, J. D., Nielsen, S. G., Horner, T. J., Ostrander, C. M. & Peterson, L. C. Thallium-

292   isotopic compositions of euxinic sediments as a proxy for global manganese-oxide burial.

293   *Geochim. Cosmochim. Acta* **213,** 291-307 (2017).

294   19. Raiswell, R. et al. The iron paleoredox proxies: a guide to pitfalls, problems and proper

295   practice. *Am. J. Sci.* **318,** 491-526 (2018).

296   20. Ostrander, C. M., Owens, J. D. & Nielsen, S. G. Constraining the rate of oceanic

297   deoxygenation leading up to a Cretaceous Oceanic Anoxic Event (OAE-2: ~94Ma). *Sci. Adv.*

298   **3,** e1701020 (2017).

299   21. Them, T. R. et al. Thallium isotopes reveal protracted anoxia during the Toarcian (Early

300   Jurassic) associated with volcanism, carbon burial, and mass extinction. *Proc. Natl. Acad.*

301   *Sci.* doi:10.1073/pnas.1803478115 (2018).

302   22. Nielsen, S. G. et al. Hydrothermal fluid fluxes calculated from the isotopic mass balance of

303   thallium in the ocean crust. *Earth and Planet. Sci. Lett.* **251,** 120-133 (2006).

304   23. Nielsen, S. G. et al. Thallium isotopic composition of the upper continental crust and rivers –

305   an investigation of the continental sources of dissolved marine thallium. *Geochim.*

306   *Cosmochim. Acta* **19,** 2007-2019 (2005).

307   24. Nielsen, S. G. et al. Towards an understanding of thallium isotope fractionation during

308   adsorption to manganese oxides. *Geochim. Cosmochim. Acta* **117,** 252-265 (2013).

309   25. Wasylenki, L. E. et al. The molecular mechanism of Mo isotope fractionation during

310   adsorption to birnessite. *Geochim. Cosmochim. Acta* **75,** 5019-5031 (2011).

311   26. Nägler, T. F. et al. Proposal for an international molybdenum isotope measurement standard

312   and data representation. *Geostand. Geoanal..Res*. doi: 10.1111/j.1751-908X.2013.00275.x

313   (2014).

314   27. Willbold, M. & Elliot, T. Molybdenum isotope variations in magmatic rocks. *Chem. Geol.*

315   **449,** 253-268 (2017).

316   28. Neubert, N., Nägler, T. F. & Böttcher, M. E. Sulfidity controls molybdenum isotope

317   fractionation into euxinic sediments: Evidence from the modern Black Sea. *Geology* **36,** 775-

318   778 (2008).

319   29. Siebert, C. et al. Molybdenum isotope fractionation in soils: influence of redox conditions,

320   organic matter, and atmospheric inputs. *Geochim. Cosmochim. Acta* **162,** 1-24 (2015).

321   30. Archer, C. & Vance, D. The isotopic signature of the global riverine molybdenum flux and

322   anoxia in the ancient oceans. *Nat. Geosci.* **1,** 597-600 (2008).

323   31. King, E. K. & Pett-Ridge J. C. Reassessing the dissolved molybdenum isotopic composition

324   of ocean inputs: The effect of chemical weathering and groundwater. *Geology*,

325   10.1130/G45124.1 (2018).

326   32. Goldberg, T., Archer, C., Vance, D. & Poulton, S. W. Mo isotope fractionation during

327   adsorption to Fe (oxyhydr)oxides. *Geochim. Cosmochim. Acta* **73,** 6502-6516 (2009).

328   33. Peacock, C. L. & Moon, E. M. Oxidative scavenging of thallium by birnessite: Explanation

329   for thallium enrichment and stable isotope fractionation in marine ferromanganese

330   precipitates. *Geochim. Cosmochim. Acta* **84,** 297-313 (2012).

331   34. Anbar, A. D. et al. A whiff of oxygen before the great oxidation event? *Science* **317,** 1903-

332   1906 (2007).

333   35. Kaufman, A. J. et al. Late Archean biospheric oxygenation and atmospheric evolution.

334   *Science* **317,** 1900-1903 (2007).

335   36. Garvin, J., Buick, R., Anbar, A. D., Arnold, G. L. & Kaufman, A. J. Isotopic evidence for an

336   aerobic nitrogen cycle in the latest Archean. *Science* **323,** 1045-1048 (2009).

337   37. Reinhard, C. T., Raiswell, R., Scott, C., Anbar, A. D. & Lyons, T. W. A late Archean sulfidic

338   sea stimulated by early oxidative weathering of the continents. *Science* **326,** 713-716 (2009).

339   38. Duan, Y. et al. Molybdenum isotope evidence for mild environmental oxygenation before the

340   Great Oxidation Event. *Geochim. Cosmochim. Acta* **74,** 6655-6668 (2010).

341   39. Kendall, B., Creaser, R. A., Reinhard, C. T., Lyons, T. W. & Anbar, A. D. Transient episodes

342   of mild environmental oxygenation and oxidative continental weathering during the late

343   Archean. *Sci. Adv.* **1**:e1500777 (2015).

344   40. Gregory, D. D. et al. The chemical conditions of the late Archean Hamersley basin inferred

345   from whole rock and pyrite geochemistry with $\Delta^{33}S$ and $\delta^{34}S$ isotope analyses. *Geochim.*

346   *Cosmochim. Acta* **149,** 223-250 (2015).

347   41. Wille, M. et al. Evidence for a gradual rise of oxygen between 2.6 and 2.5 Ga from Mo

348   isotopes and Re-PGE signatures in shales. *Geochim. Cosmochim. Acta* **71,** 2417-2435 (2007).

349   42. Algeo, T. J. and Tribovillard, N. Environmental analysis of paleoceanographic systems based

350   on molybdenum-uranium covariation. *Chem. Geol.* **268,** 211-225 (2009).

351   43. Johnson, J. E. et al. Manganese-oxidizing photosynthesis before the rise of cyanobacteria.

352   *Proc. Natl. Acad. Sci.* **110,** 11238-11243 (2013).

353   44. Anbar, A. D. & Holland, H. D. The photochemistry of manganese and the origin of banded

354   iron formations. *Geochim. Cosmochim. Acta* **56,** 2595-2603 (1992).

355   45. Kendall, B, Dahl, T. W. & Anbar, A. D. Good golly, why Moly? The stable isotope

356   geochemistry of molybdenum. *Rev. Mineral. Geochem.* **82,** 682-732 (2017).

357   46. Nielsen, S. G., Rehkämper, M. & Prytulak, J. Investigation and application of thallium

358   isotope fractionation. *Rev. Mineral. Geochem.* **82,** 759–798 (2017).

359   47. Holland, H. D. *The chemical evolution of the atmosphere and oceans* (Princeton Univ. Press,

360   Princeton, NJ, 1984).

361   48. Habicht, K. S., Gade, M., Thamdrup, B., Berg, P. & Canfield, D. E. Calibration of sulfate

362   levels in the Archean ocean. *Science* **298,** 2372-2374 (2002).

363   49. De Kock, M. O., Evans, D. A. D. & Beukes, N. J. Validating the existence of Vaalbara in the

364   Neoarchean. *Precambr. Res.* **174,** 145-154 (2009).

365   50. Madison, A. S., Tebo, B. M., Mucci, A., Sundby, B. & Luther III, G. W. Abundant porewater

366   Mn(III) is a major component of the sedimentary redox system. *Science* **341,** 875-878 (2013).

367

368   [*]correspondence to: cmostran@asu.edu

369

380

381 **Author contributions:** C.M.O., S.G.N., J.D.O., B.K., and A.D.A. developed the project idea.

382 C.M.O. processed samples and performed Tl and Mo isotope analyses with contributions from

383 S.G.N., J.D.O., B.K., G.W.G., and S.J.R.. C.M.O. performed the modeling and wrote the

384 manuscript with contributions from all co-authors.

385

386 **Data Availability:** All data generated during this study are included in the supplementary

387 information.

388

389 **Competing interests:** The authors declare no competing interests.

390

391 **Figure Captions:**

392 **Figure 1. Illustration of a possible well-oxygenated marine margin before the GOE.**

393 Evidence exists for sufficient O_2 accumulation in an ancient water column between 2.6 and 2.5

394 Ga to weakly oxygenate underlying sediments[3] ("suboxic"; Panel A). However, O_2 penetration

395 into these sediments was not sufficient to promote Mn oxide burial[11,12]. If settings capable of

396 burying Mn oxides were present in ancient oceans ("oxic"; Panel B) over a large seafloor area,

397 then seawater Tl and Mo isotope compositions would have decreased and increased,

398 respectively. The Mt. McRae Shale was deposited under locally euxinic conditions[37] and should

399 therefore have captured these changes in seawater isotope signatures[18,28]. Sedimentary redox

400 structure is modified from previous work[50].

401

402   **Figure 2. Geochemical profiles in organic-rich shales from the Mt. McRae Shale (orange =**

403   **ϵ^{205}Tl, blue = δ^{98}Mo).** Hatched boxes represent values indicative of anoxic ($Fe_{HR}/Fe_T > 0.22$)

404   and euxinic ($Fe_{Py}/Fe_{HR} > 0.7$) deposition[19]. Data that exceed both criteria are in black. Diamonds

405   reflect data from previous work[37,38] and circles are data from this study. The grey vertical line in

406   the isotope plot represents average isotope compositions from the lower shale member, with the

407   exception of one anomalous Tl isotope value (ϵ^{205}Tl = -4.28 ± 0.13 at 180.33 m). All error bars

408   represent the 2SD reproducibility of that sample or the external long-term reproducibility of

409   natural reference materials, whichever is greater.

410

411   **Figure 3. Mo and Tl isotope cross-plot from the upper shale member.** The anti-correlation

412   trend in this plot, which is also apparent in Figure 1, is statistically significant (*p*-value = 0.01).

413   The brown box indicates current estimates for the isotope compositions of bulk continental

414   crust[23,27]. All error bars represent the 2SD reproducibility of that sample or the external long-

415   term reproducibility of natural reference materials, whichever is greater.

416

417   **Methods:**

418   <u>Tl isotopes</u>

419   Tl sample preparation and purification were performed in the NIRVANA Laboratory at

420   Woods Hole Oceanographic Institution (WHOI), as well as in Dr. Jeremy Owens' Laboratory at

421   Florida State University (FSU) within the National High Magnetic Field Laboratory (NHMFL).

422   Powdered samples from ABDP9 were leached using a method from previous literature[17,20],

423   which has been shown to effectively separate authigenic Tl (i.e. Tl bound to pyrite) from detrital

424 Tl. Each fraction was subsequently digested following procedures discussed in that literature. Ion

425 exchange chromatography was completed using previously described techniques[51,52]. Similar to

426 recent work[20], samples were only subjected to one column pass because Tl concentrations were

427 high and thus very little sample mass was processed.

428   Tl isotopic analyses were conducted at the WHOI Plasma Mass Spectrometry Facility

429 and at the NHMFL in Tallahassee. At both locations a Thermo Neptune MC-ICPMS was used

430 with an Aridus II desolvating nebulizer sample introduction system. Measurements were made in

431 low-resolution mode utilizing sample-standard bracketing relative to NIST 997 Tl in epsilon

432 notation. External normalization to NIST SRM 981 Pb was utilized to monitor instrumental mass

433 bias, similar to previous studies[51,52]. Since a known quantity of NIST SRM 981 Pb was added to

434 each sample, Tl concentrations could be calculated during MC-ICPMS analysis using the

435 measured $^{205}Tl/^{208}Pb$ ratios. Tl isotope values are reported in epsilon notation relative to NIST

436 997 Tl metal. One USGS shale SCO-1 standard was leached, purified, and analyzed with each

437 sample set to monitor accuracy and showed good reproducibility ($\varepsilon^{205}Tl_{authigenic}$ = -2.80 ± 0.13,

438 2SD, n = 8) compared to a recent study:(-2.92 ± 0.11)[20].

439

440 <u>Mo isotopes</u>

441   All Mo sample digestion, isotope purification, and analysis were completed at the W.M.

442 Keck Foundation Laboratory for Environmental Biogeochemistry at Arizona State University.

443 Quarter cores were cut from ABDP9, powdered, ashed, digested, and concentrations were

444 analyzed using the same techniques employed in previous work[34]. Enough sample was then

445 taken from the same digested stock solutions to provide 125 ng Mo that was spiked with an

446 optimal amount of calibrated synthetic Mo isotope double-spike (^{97}Mo and ^{100}Mo) before

447 purification via ion exchange chromatography, again utilizing methods from previous

448 studies[53,54]. The double spike is used for chromatography and instrumental mass fractionation

449 correction.

450   Isotope ratio measurements were performed on a Thermo Neptune multi-collector

451 ICPMS (MC-ICPMS) in low-resolution mode with an Elemental Scientific Inc. Apex inlet

452 system and using sample-standard bracketing[38,55]. All measurements were made using the

453 Johnson Matthey Specpure Mo plasma standard (Lot #802309E; RochMo2) as the bracketing

454 standard, and then re-calculated relative to the new international NIST SRM 3134 standard = +

455 0.25‰[(26)]. Samples and standards were analyzed at a concentration of 25 µg/g Mo, which

456 yielded about three volts of signal on mass 98. Samples were analyzed in triplicate (at least),

457 with the average 2SD sample reproducibility being 0.06‰, and the maximum being 0.11‰.

458 Over the 12-month period of Mo isotope analysis for this study, USGS rock reference material

459 SDO-1 was simultaneously processed with each batch of samples to monitor accuracy and

460 showed good reproducibility (δ^{98}Mo = 1.00 ± 0.09‰ 2SD compared to 1.05 ± 0.14‰ from a

461 previous study[56]), as did various analytical replicates (Table 1). Lastly, for each analytical run, a

462 series of standards with varying spike-sample ratios was measured. All samples were within the

463 validated spike-sample range for accurate and precise δ^{98}Mo values.

464

Table 1. Standard solution δ^{98}Mo values from this study vs. previous work

Standard	This study[a]	n	Normalized to NIST + 0.25‰[b]	Goldberg et al. (2013)
Roch-Mo2	Bracketing std.		-0.09‰	-0.09 ± 0.05‰
ICL-Mo	0.16 ± 0.03‰	38	0.07 ± 0.03‰	0.09 ± 0.05‰

Kyoto-Mo	-0.04 ± 0.05‰	39	-0.13 ± 0.05‰	-0.12 ± 0.06‰
NIST SRM 3134	0.33 ± 0.06‰	45	0.24 ± 0.06‰	0.25‰ (reporting std.)
SDO-1	1.12 ± 0.05‰	45	1.03 ± 0.05‰	1.05 ± 0.14‰

a. Measured relative to Roch-Mo2

b. Normalized using $\delta^{98}Mo_{Roch-Mo2}$ = -0.09‰ relative to $\delta^{98}Mo_{NIST+0.25‰}$[56]

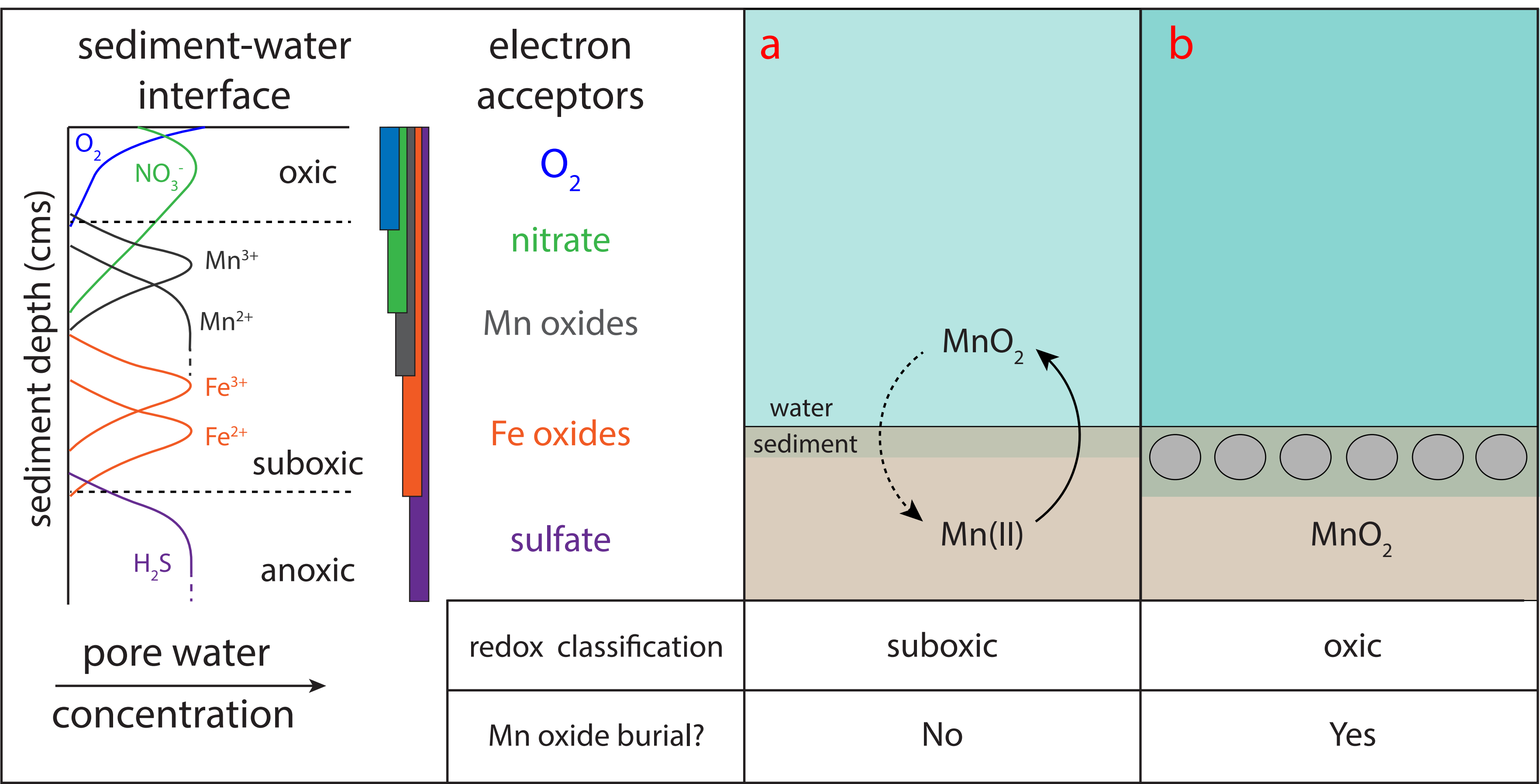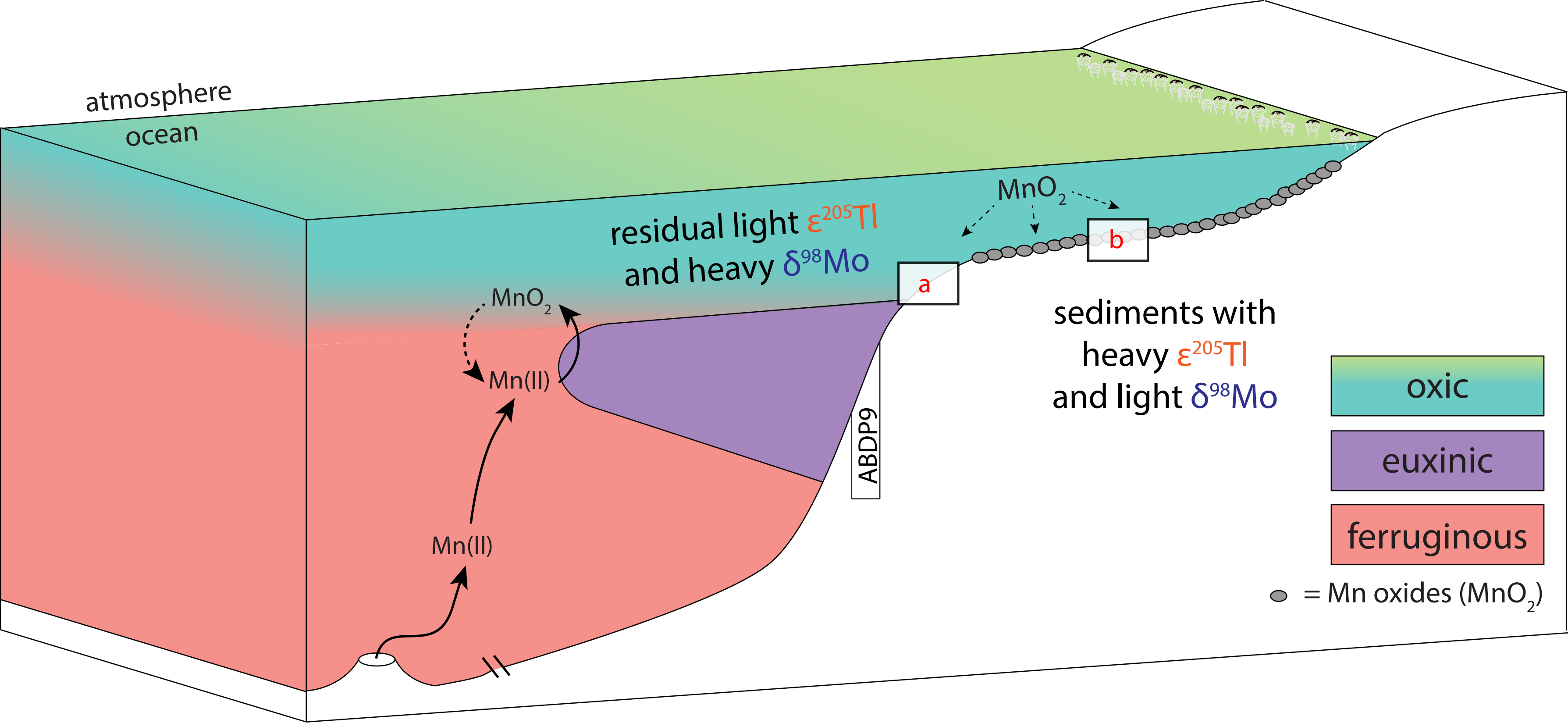*all reported errors are 2SD of the standard reproducibility

465
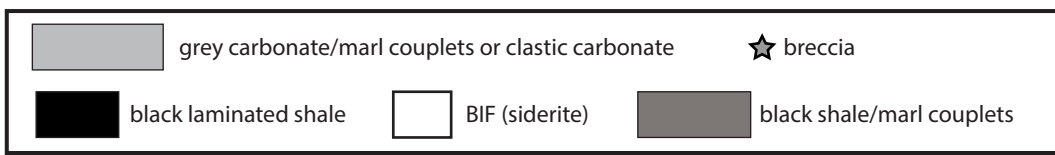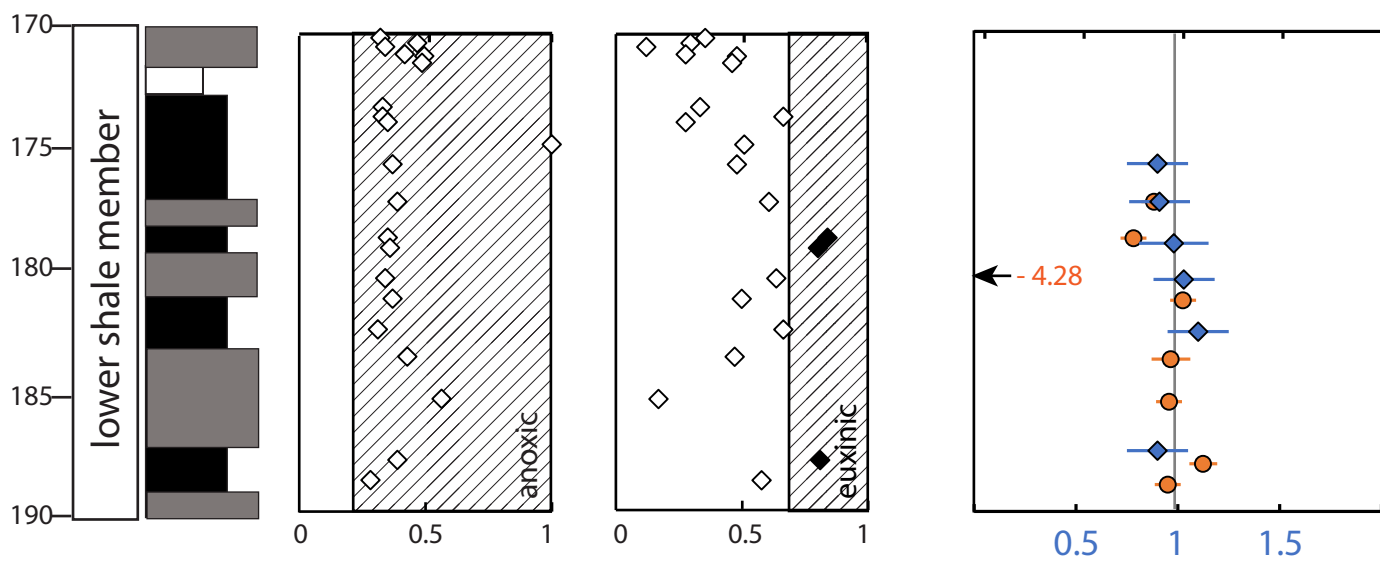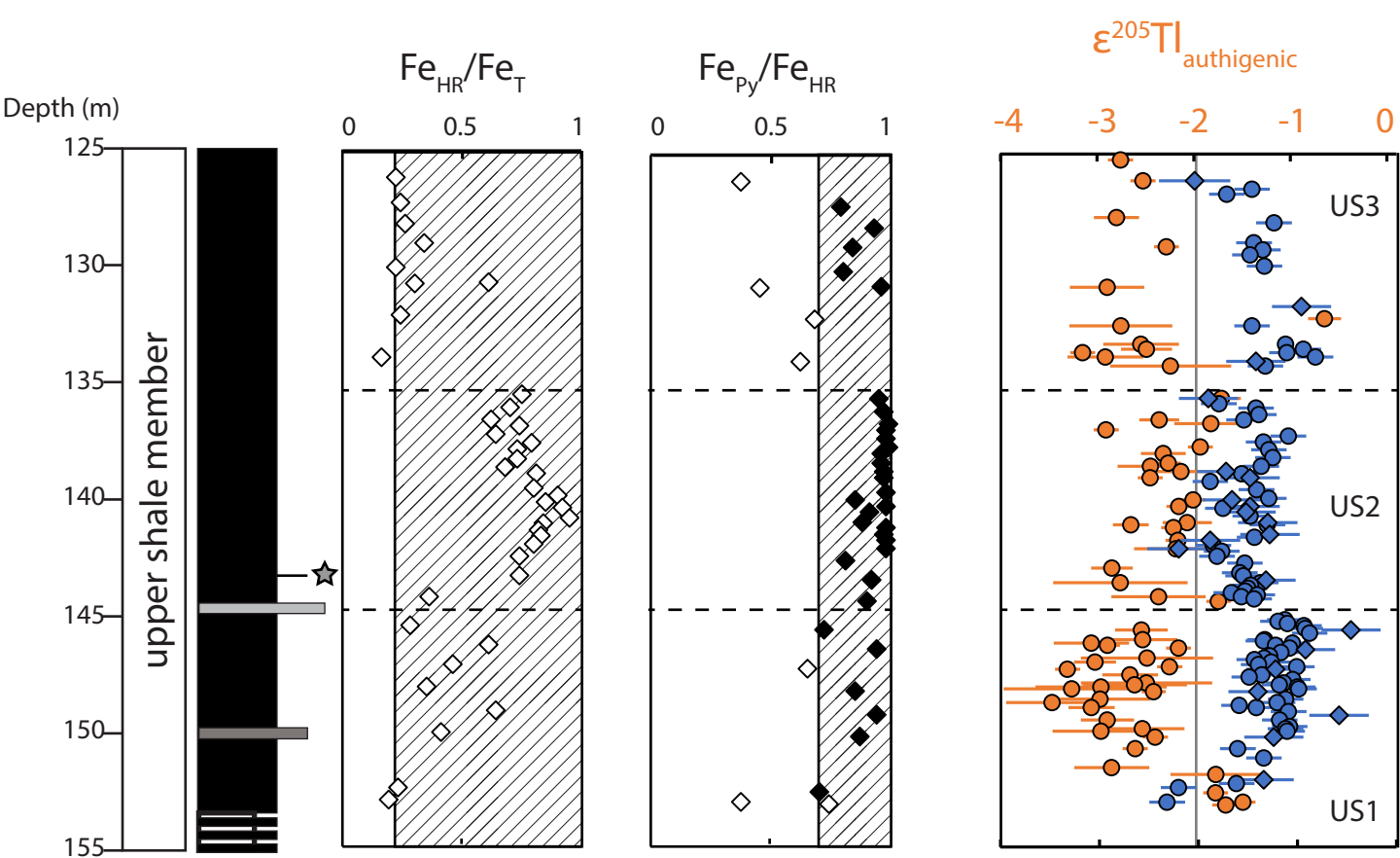
466 **References cited only in Methods:**

467 51. Rehkämper, M. & Halliday, A. N. The precise measurement of Tl isotopic compositions by

468   MC-ICPMS: Applications to the analysis of geological materials and meteorites. *Geochim.*

469   *Cosmochim. Acta* **63,** 935-944 (1999).

470 52. Nielsen, S. G., Rehkämper, M., Baker, J. A. & Halliday, A. N. The precise and accurate

471   determination of thallium isotope compositions and concentrations for water samples by MC-

472   ICPMS. *Chem. Geol.* **204,** 109-124 (2004).

473 53. Siebert, C., Nägler, T. F. & Kramers, J. D. Determination of the molybdenum isotope

474   fractionation by double-spike multicollector inductively coupled plasma mass spectrometry.

475   *Geochem. Geophys. Geosyst.* 2:2000GC000124 (2001).

476 54. Barling, J., Arnold, G. L. & Anbar, A. D. Natural mass-dependent variations in the isotopic

477   composition of molybdenum. *Earth and Planet. Sci. Lett.* **193,** 447-457 (2001).

478 55. Kendall, B., Creaser, R. A., Gordon, G. W. & Anbar, A. D. Re-Os and Mo isotope

479   systematics of black shales from the Middle Proterozoic Velkerri and Wollogorang

480   Formations, McArthur Basin, northern Australia. *Geochim. Cosmochim. Acta* **73,** 2534-2558

481   (2009).

482 56. Goldberg, T. et al. Resolution of inter-laboratory discrepancies in Mo isotope data: an

483   intercalibration. *J. Anal. At. Spectrom.* **28,** 724-735 (2013).

Top diagram labels:

atmosphere
ocean

residual light $\varepsilon^{205}Tl$
and heavy $\delta^{98}Mo$

MnO_2

sediments with
heavy $\varepsilon^{205}Tl$
and light $\delta^{98}Mo$

MnO_2

Mn(II)

Mn(II)

a

b

ABDP9

| oxic |
| euxinic |
| ferruginous |

● = Mn oxides (MnO_2)

Bottom diagram labels:

sediment-water
interface

electron
acceptors

a   b

O_2

NO_3^-

oxic

Mn^{3+}

Mn^{2+}

Fe^{3+}

Fe^{2+}

suboxic

H_2S

anoxic

O_2

nitrate

Mn oxides

Fe oxides

sulfate

pore water
concentration

sediment depth (cms)

water
sediment

MnO_2

Mn(II)

MnO_2

	a	b
redox classification	suboxic	oxic
Mn oxide burial?	No	Yes

Legend:

- grey carbonate/marl couplets or clastic carbonate
- ⭐ breccia
- black laminated shale
- BIF (siderite)
- black shale/marl couplets